Neurochemical Research (2025) 50:169
https://doi.org/10.1007/s11064-025-04421-y

RESEARCH

Neuroplasticity After Hypoxic-Ischemic Brain Injury in Neonatal Pigs Based on Time-Dependent Behavior of ^{1}H-MRS-Tau Protein and Synaptic Associated Proteins and Synaptic Structure Analysis

Sijia Zhao[1] · **Yang Zheng**[1]

Received: 18 December 2024 / Revised: 9 May 2025 / Accepted: 12 May 2025

Abstract

This study investigated the effects of hypoxic-ischemic (HI) injury on neonatal neuroplasticity using the following approaches: Magnetic Resonance Spectroscopy (^{1}H-MRS) imaging to analyze dynamic changes in tau protein levels, immunofluorescence staining to evaluate synaptophysin (SYP), neurocan (Neu), and tau protein, and utilizing transmission electron microscopy (TEM) to examine synaptic ultrastructure at multiple time points. A total of 59 healthy neonatal pigs were included, with 10 in the control group and 43 in the HI model group. The results demonstrated that SYP immunostaining intensity peaked at 6–12 h after HI before declining. Neu expression exhibited an initial decrease, followed by a transient increase and subsequent reduction, reaching its lowest level at 6–12 h after HI. Tau protein levels increased initially after HI, peaked at 24–48 h after HI, and subsequently decreased. SYP was negatively correlated with Neu with a correlation coefficient of -0.877. SYP was not correlated with Tau, neither was Neu with Tau. Compared with the control group, the number of synaptic vesicles decreased, and Post-Synaptic Density (PSD) thickness increased 6–12 h after HI. At 12–24 h after HI, the number of synaptic vesicles increased, and PSD thickness slightly decreased. At 24–48 h after HI, the vesicle number decreased, PSD became thinner, interrupting continuity, mitochondria swelled, and mitochondrial cristae blurred and disappeared. The findings suggest that the expression of Tau, SYP, and Neu is linked to alterations in synaptic and myelin structures, reflecting varying aspects of neural plasticity following HI injury.

Keywords Synapse · Plasticity · Synaptophysin · Neurocan · PSD

Introduction

The brains of newborns are more adaptable to external stimuli than those of adults. After hypoxic ischemia (HI), nerve cells and neural networks will undergo adaptive changes to maintain body homeostasis; this inherent characteristic of the central nervous system (CNS) is known as neural "plasticity" [1, 2]. Previous H&E (Hematoxylin and Eosin) staining in our lab revealed time-dependent histopathological changes in the basal ganglia of neonatal pigs post-HI: glial cell swelling with cytoplasmic pallor at 6 h, neuronal swelling with pyknosis at 24 h, scattered neuronal necrosis at 48 h, and membrane rupture/nuclear swelling at 72 h. Both astrocytes and neurons exhibited progressively severe damage over HI duration [3]. Mild to moderate injury can trigger neuroprotective mechanisms to adapt to the pathological state of the nervous system. The extension of axons needs to be covered with myelin sheath to ensure rapid and accurate electrophysiological communication to target cells. After severe or prolonged injury, the structure and function of axons, myelin sheath, and synapses will be damaged, and the dynamic imbalance of the brain microenvironment will reduce plasticity, causing cognitive dysfunction [4].

Synapses are formed by neurons and mediate information transmission, and underlie the physiological functions of neural networks. Synaptic connections are important structures for information and material transmission among

✉ Yang Zheng
zhengyang19871114@163.com

Sijia Zhao
zsj928966389@gmail.com

[1] Department of Radiology, Shengjing Hospital of China Medical University, No. 36, Sanhao Street, Heping District, Shenyang 110004, PR China

Published online: 23 May 2025

neurons [5]. The number and structural integrity of synapses play an important role in maintaining normal brain function [6]. After HI injury, synapses can adapt to changes in the brain microenvironment by changing their structure and function [7, 8], including changes in size, morphology and synaptic related protein expression, which mainly depend on the dynamic balance of synapse related protein synthesis and degradation [7, 9–11]. Synapses are composed of presynaptic components, synaptic cleft, and postsynaptic membrane. Presynaptic components include mitochondria, microtubules, microfilaments, and a large number of synaptic vesicles, which store and release neurotransmitters. Thus, axons, myelin sheaths, and synaptic connections work together for neurotransmitter and signaling activities. Synaptic plasticity is an important component of brain plasticity, including the regulation of molecular and cellular levels and physiological changes. Synaptic plasticity promotes the brain to change its organizational structure and function according to different states, and can keep the nervous system in dynamic change [12]. After HI injury, synapses can adapt to changes in the brain microenvironment by changing their structure and strength. Synaptic reconstruction is a necessary process in the recovery of brain function after HI injury. The reconstruction involves synaptic related proteins, axon regeneration and changes to synaptic structures. Synaptophysin (SYP) is a specific marker protein localized to presynaptic terminals, predominantly distributed on the membranes of synaptic vesicles (SVs). It regulates SV formation and recycling, while SVs are primarily located at presynaptic terminals and function in the storage and release of neurotransmitters [13]. SYP is involved in the modulation of calcium ion dynamics, including Ca^{2+} binding, neurotransmitter release, and synaptic vesicle recruitment. SYP is involved in synapse formation and stability and can reflect synapse density, distribution, and functional state. It can be used as a landmark molecule reflecting the repair mechanism after nerve injury, thus reflecting synaptic plasticity [14, 15]. Neurocan (Neu) is a specific protein secreted by neurons and glial cells, involved in the development of the CNS and nerve repair, and closely related to pathophysiological processes such as glial scar formation and axon growth inhibition [16]. Excitatory synapses are characterized by the morphological and functional specialization of the postsynaptic membrane, known as Post-Synaptic Density (PSD). Under electron microscopy, the PSD appears as a layer of electron-dense material on the cytoplasmic surface of the postsynaptic membrane, primarily composed of receptors, scaffolding proteins, and other components [17].

Myelination is key for the development of the nervous system. As an insulating layer, the myelin sheath wraps around neuronal axons and ensures their normal and rapid electrical conduction. Tau protein is a microtubule-associated protein expressed in neurons and oligodendroglia (OL). Compared with the mature brain, in the developing brain, Tau presents special phosphorylation [18, 19] and is involved in regulating myelination. During neurite growth, the neuron cell body must synthetize numerous substances, and the cell morphology must remain stable, which requires a firm cytoskeleton. Microtubules, a protein-based cytoskeletal structure in the neurite, maintains the morphological stability of differentiated neurons, while serving as a transport route for various proteins and organelles to the neurite. Tau protein mainly plays a role in maintaining the stability of formed microtubules, contributing to microtubule elongation and participating in physiological processes such as intracellular material transport, mitosis, and neurotransmitter and signal transmission, an important factor in maintaining microtubule stability. During myelination, “Fyn-Tau-MT” binding plays an important role in OL differentiation [20]. Axon-derived signals are recognized by OL membrane receptors and activate Fyn, which regulates OL proliferation and differentiation and MBP synthesis. MBP is the main protein of the myelin sheath in the mature CNS. Pathological Tau modification after HI reduces the binding ability of “Fyn-Tau-MT” blocking downstream signal transduction pathway, resulting in impaired myelination [21]. MBP mRNA is contained in RNA transport particles, bound with Tau and transported to the plasma membrane of OL by MT transport; MBP is synthesized under Fyn regulation. Pathological Tau phosphorylation leads to decreased MT stability and affect the transport of MBP RNA transport particles, thus affecting myelin sheath formation. Simultaneously, abnormal Tau phosphorylation can cause mitochondrial dysfunction and lead to energy metabolism disorders in OL and neurons. Pathological Tau protein expression and abnormal phosphorylation are important factors affecting myelination after HI.

In this study, the axon-myelin sheath, synaptic-associated proteins, and synaptic structure after HI were investigated as a dynamic whole. By detecting protein expression of the above indicators and the synaptic structure changes at various time points after HI, we evaluated neuroplasticity after HI.

Materials and Methods

Experimental Animals

A total of 59 healthy newborn piglets (Large White Pigs, namely Yorkshire Piglets), regardless of sex, were selected 3–5 days after birth, weighing 1–1.5 kg. Among them, 30 were male and 43 were female. A total of 53 cases were included for data analysis, excluding six cases of mid-course

death, modeling failure, and motion artifact. They were randomly assigned to control group ($n=10$) and model group ($n=43$). The model group was further divided into 6 time periods according to magnetic resonance (MR) scanning time after Hypoxic-Ischemic Brain Injury (HIBI) (0–2 h, $n=8$; 2–6 h, $n=8$; 6–12 h, $n=6$; 12–24 h, $n=10$; 24–48 h, $n=5$; 48–72 h, $n=6$). All experimental animals were provided by the Animal Laboratory of our institute, and the research complied with the standards stipulated in the Regulations on the Management of Experimental Animals and the Management of Experimental Animal License (Ethical Code: 2022PS250K).

Control Group

The indoor temperature was maintained at 28–30 °C, and an intramuscular injection of SuMianXin (a compound preparation consisting of 2,4-dimethylthiazole, ethylenediaminetetraacetic acid (EDTA), dihydroetorphine hydrochloride, and haloperidol; administered at 0.6 mL/kg; Veterinary Research Center, Jilin University, Changchun, China) was given. In this formulation, xylazine hydrochloride acts as a central nervous system inhibitor by activating α2 presynaptic receptors to suppress norepinephrine release; dihydroetorphine hydrochloride serves as a potent μ-receptor agonist with morphine-like analgesic effects; and haloperidol provides sedation and muscle relaxation. Tracheal intubation (diameter: 2.5 mm) was connected to a TKR-200 C small animal ventilator (Jiangxi Teli Anaesthesia & Respiration Equipment Co., Ltd), in mechanical ventilation mode, with 100% oxygen ventilator parameters: breathing ratio (I/E) 1:1.5, breathing rate: 30 times/min, pressure: 0.05–0.06 mpa. The TuffSat Palm Oximeter (GE, USA) was used to monitor the heart rate and oxygen saturation. The jugular vein was catheterized and fixed. The neck skin was disinfected with iodophor, a median incision performed, the bilateral common carotid arteries were separated, and the incision was sutured. The incision was carefully wrapped with thick cotton during surgery, and immediately placed in an incubator after modeling (Shenzhen Reward Life Technology Co. Ltd. 912-005). The rectal temperature was maintained between 39 °C and 40°C.

Model Group

The neonatal pig model group underwent the same procedure as above. After the condition stabilized after 30 min, the blood flow of bilateral common carotid arteries was blocked by arterial clamp, and 6% oxygen (Dalian Special Gases Co. Ltd.) provided by mechanical ventilation. This state was maintained for 40 min; then, the ventilator was connected to a 100% oxygen cylinder (Dalian Special Gases Co., Ltd.), and the oxygen flow rate was adjusted to 2–4 L/min with a tidal volume of 5 mL/kg, ensuring the final inspired oxygen concentration was maintained between 30% and 40%. Simultaneously, bilateral carotid artery blood supply was restored, and the incision was sutured. Blood oxygen saturation and heart rate were monitored throughout the process. The ventilator was stopped after spontaneous breathing resumed. The pigs were placed into an incubator immediately thereafter (Shenzhen Reward Life Technology Co. Ltd. 912-005).

Immunofluorescence Assay

After establishing the model, we promptly removed the brain tissue. The extracted brain hemispheres were fixed in 10% neutral formalin for 24–48 h. The tissues were then processed for embedding, ensuring that the tissue thickness did not exceed 5 mm. The tissue embedding molds were placed into a dehydrator for dehydration and paraffin infiltration. Gradual dehydration was performed using graded ethanol (70%, 80%, 90%, 95%, and 100%), with each step lasting 1 h; xylene was used for clearing for 1 h. The paraffin-infiltrated samples were removed and placed into an embedding machine (Leica, HistoCore Arcadia H, Germany), and the embedded tissues were allowed to cool for future use. The paraffin blocks were then retrieved and loaded onto a microtome (HM340E, Thermo Scientific, MI, USA) for sectioning coronally at a thickness of 4 micrometers. Layers containing the basal ganglia were collected for immunofluorescence staining of SYP, Neu, and Tau. The staining procedure was as follows: after deparaffinization in xylene and hydration through a graded ethanol series, antigen retrieval was performed by heating the sections in citrate buffer (0.01 M, pH = 6.0) in a microwave for 7 min at high temperature. Non-specific antibody binding was blocked with normal goat serum at room temperature for 30 min. Primary antibodies, including Anti-Synaptophysin antibody (1:50, ab52636, Abcam), Anti-Neurocan antibody (1:50, ab277525, Abcam), and Anti-Tau antibody (1:50, ab109390, Abcam), were incubated overnight at 4 °C. Subsequently, the sections were incubated with the secondary antibody, goat anti-rabbit IgG (Alexa Fluor® 488, 1:200, ab150077, Abcam), at room temperature for 4 h. Finally, the sections were incubated with DAPI (4',6-diamidino-2-phenylindole dihydrochloride, ab104139) for 5 min for nuclear staining. Images were acquired using a confocal microscope (Zeiss LSM880, Germany). Immunofluorescence staining of SYP, Neu, and Tau was quantified by two pathologists. The optical density (OD) values of immunofluorescence images were analyzed and observed under a microscope at 400× magnification. The above indicators were observed in five fields of view in each basal ganglia region, and data

from all five fields were integrated to analyze the Immunostaining of SYP, Neu, and Tau in different brain regions across groups at various time points.

Transmission Electron Microscopy

After removing the brain tissues, fresh basal ganglia-containing brain tissues were collected and fixed in 2.5% glutaraldehyde solution at 4 °C for >24 h (all samples were sectioned within 48 h, though epoxy resin-embedded tissue blocks could be stably stored for approximately 1 month), followed by fixation in 1% osmium tetroxide solution for 2 h. After fixation, the tissues were rinsed with distilled water, dehydrated through a graded series of ethanol and acetone, and embedded in epoxy resin. The embedded tissues were dried and stored in a thermostatic chamber. The tissue blocks were trimmed and sectioned into ultra-thin 70 nm grids using a Leica EM UC7 ultramicrotome (Leica, Wetzlar, Germany). The sections were first stained with uranyl acetate for 10 min, then with lead citrate for 5 min, and finally rinsed with distilled water. After air-drying, the sections were observed under a transmission electron microscope (TEM) (JEM-1400Flash, Japan). Initially, five fields of view were captured at ×2000 magnification. Subsequently, two random images were taken for each field at ×8000 and ×10,000 magnifications, respectively. For each group of animals, >50 synapses were evaluated. Image acquisition and TEM evaluation were performed by two pathologists.

Treatment After ^{1}H-MRS

A Philips 3.0T MRI (Achieva 3.0T TX; Philips Healthcare Systems, Best, the Netherlands) was used for scanning with pen beam and second-order uniform field, transmitted by body coil and received by eight-channel head coil (SENSE). MRS adopted single-voxel long TE scanning: TR/TE = 2000/144 ms, NSA = 64, VOI = 10 × 10 × 10 mm^3. Regions of interest (ROIs) were selected in the right base segment. Each neonatal pig underwent MR scan at all time points specified in the grouping after HI. The spectral data obtained by scanning were post-processed by linear combination of Model in Vitro Spectra (LcModel) (NAA at 2.02 ppm, Cr at 3.02 ppm, Cho at 3.2 ppm, Lac at 1.33 PPM and Tau peaks around 3.25 and 3.42 ppm.)

Statistical Analyses

The optical density value (OD value) of immunofluorescent images was analyzed and observed under 400× magnification with a microscope. The higher OD value, the higher immunostaining. Image J software (Java 1.6.0; National Institutes of Health, USA) was used for immunostaining image analysis. The data from ^{1}H MRS is processed and analyzed using LcModel. Statistical analysis software SPSS for Windows (Version 17.0, Chicago, IL) was used for data processing; measurement data are expressed as mean ± standard deviation (mean ± SD). The Levene test was applied to test the normal distribution and homogeneity of variance of the data in each group. One-way ANOVA were used to compare the total differences. Tukey's *post hoc* test was used for *post hoc* tests among multiple groups. Dunnett's *t*-test was used for groups with unequal variances. Spearman rank correlation analysis was used to test the correlation. $P < 0.05$ was considered statistically significant. *$P < 0.05$, **$P < 0.001$.

Results

SYP Immunostaining After HI

SYP immunostaining intensity initially increased after HI, peaked at 6–12 h, and subsequently declined. One-way ANOVA revealed significant intergroup differences over time ($P < 0.05$). Post hoc tests confirmed that the most pronounced changes occurred in the 6–12 h post-HI group compared to controls ($P < 0.05$), as shown in Fig. 1.

Neu Immunostaining Changed After HI

We found that after HI, Neu immunostaining first decreased, then increased, later decreasing. One-way ANOVA indicated significant intergroup differences in Neu staining over time ($P < 0.05$). Post hoc analysis revealed that the 6–12 h after HI, which exhibited the lowest Neu staining levels, showed statistically significant differences compared to the control group ($P < 0.001$), as demonstrated in Fig. 2.

Time-Dependent Changes of Tau Protein After HI

Both ^{1}H-MRS and immunostaining results showed that Tau protein levels peaked at 24–48 h post-HI, with significant differences compared to controls ($P < 0.05$) in post hoc tests. One-way ANOVA confirmed overall group differences ($P < 0.05$). Post hoc comparisons of ^{1}H-MRS data revealed significant differences between the 24–48 h and 48–72 h post-HI groups ($P < 0.05$), as shown in Fig. 3.

Correlation Between SYP, Neu, and Tau Protein Immunostaining After HI

After HI, SYP initially increased and then decreased, while Neu exhibited an initial decrease, followed by an increase,

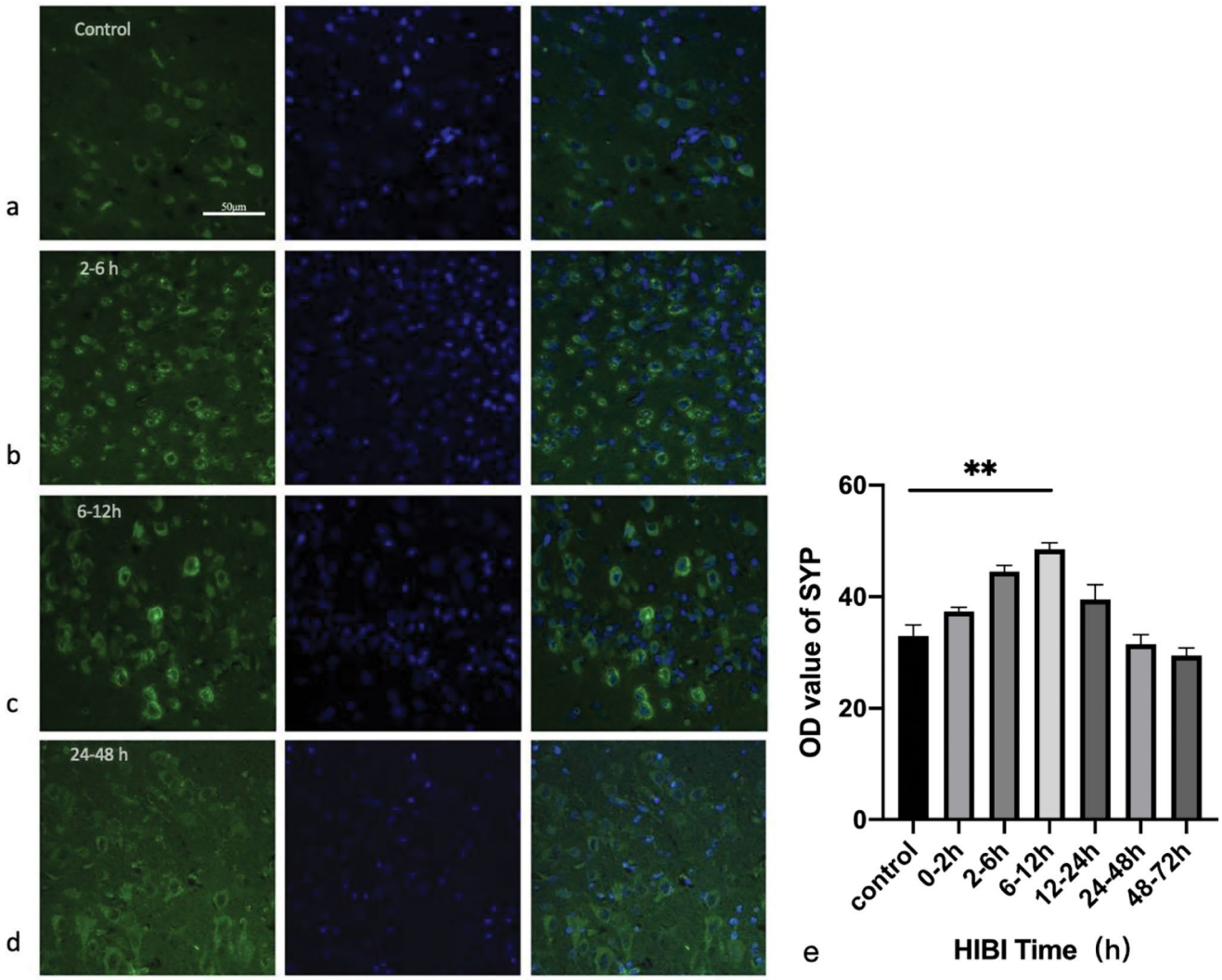

Fig. 1 Changes in SYP protein immunostaining in the basal ganglia region of the control group and at some time points after HI (400×). SYP protein immunostaining in the control group (**a**) and at 2–6 h (**b**), 6–12 h (**c**), and 24–48 h (**d**) after HI. Left: SYP on the cell membrane (green); middle: cell nuclei (DAPI, blue); right: merged image showing target protein on the cell membrane and nuclei. SYP exhibited an initial increase followed by a decrease after HI, with the peak at 6–12 h after HI. Comparison between the control group and the 6–12 h after HI group (**e**). *$P<0.05$, ** $P<0.001$

and then a subsequent decrease. A significant negative correlation was observed between SYP and Neu (r = -0.877, $P<0.001$). However, no correlation was found between SYP and Tau ($P=0.229$) or between Neu and Tau ($P=0.342$), as shown in Fig. 4.

Synaptic Structural Changes in the Basal Ganglia Region After HI

Compared with the control group, the number of synaptic vesicles decreased and postsynaptic dense area (PSD) thickness increased 6–12 h after HI (it refers to a homogeneous layer of dense material with high electron density on the cytoplasmic surface of the inner side of the postsynaptic membrane under electron microscopy, and its thickness that of dense material), and normal mitochondrial structures were observed. In the 12–24 h group, the mitochondrial cristae were blurred and the mitochondria swollen. The number of synaptic vesicles increased and PSD thickness slightly decreased. At 24–48 h, the number of vesicles and mitochondria decreased, PSD thinner, continuity was interrupted, and the synaptic cleft widened. In the control group, the myelin sheath was smooth and uniform; after HI, the myelin sheath was uneven and continuity interrupted, as part of the myelin sheath thinned out and disappeared, as shown in Figs. 5 and 6.

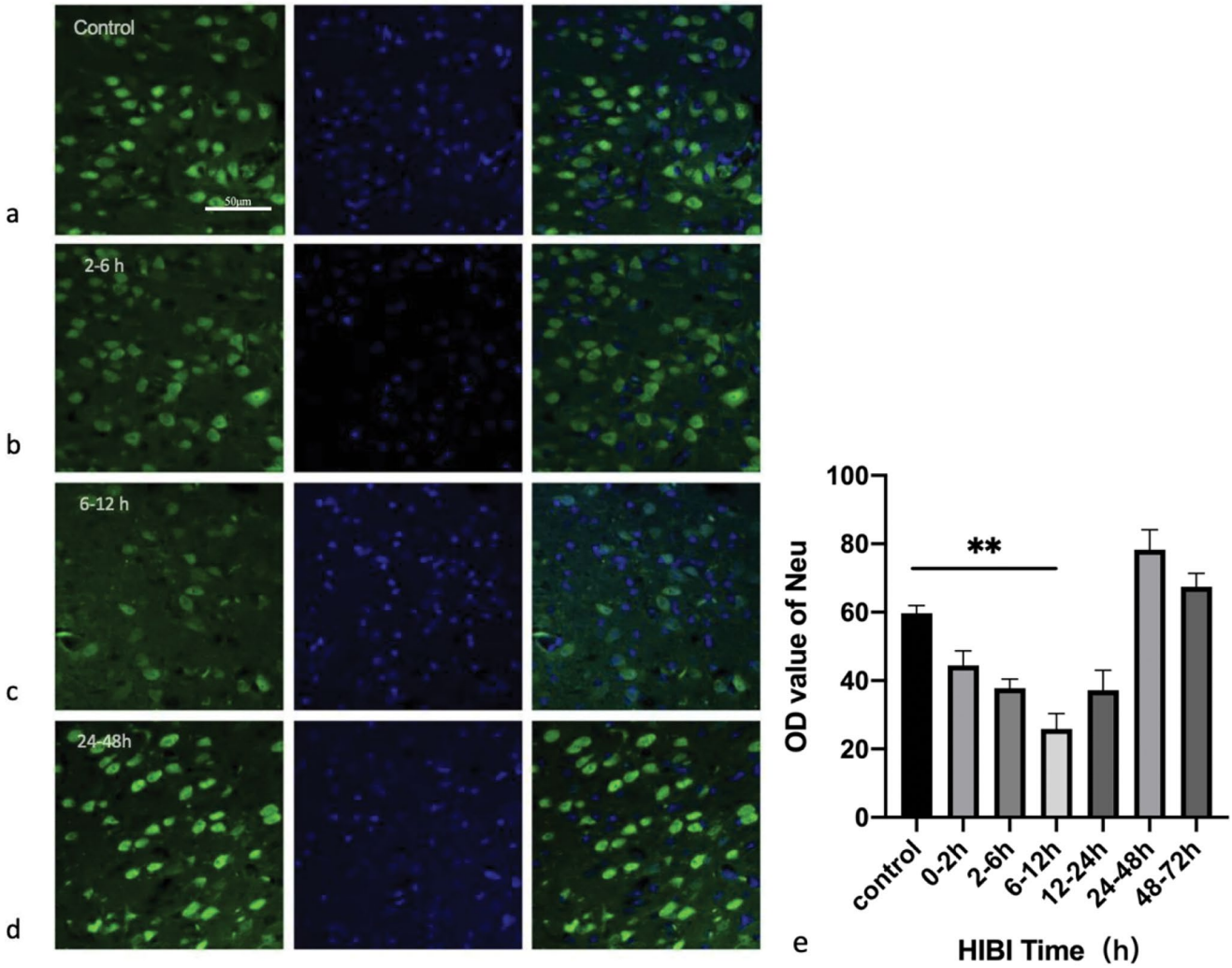

Fig. 2 Changes in Neu immunostaining in the basal ganglia region of the control group and at some time points after HI (400×). Neu immunostaining in the control group (**a**) and at 2–6 h (**b**), 6–12 h (**c**), and 24–48 h (**d**) after HI. Left: Neu on the cell membrane (green); middle: cell nuclei (DAPI, blue); right: merged image showing target protein on the cell membrane and nuclei. Immunostaining revealed that Neu was lowest at 6–12 h after HI ($P<0.001$) (**e**). * $P<0.05$, ** $P<0.001$

Discussion

Presynaptic components influence synaptic density through the content released by synaptic vesicle exocytosis and the number of sensors in each synaptic vesicle [22–24]. SYP is a glucose-containing structural protein on the membrane of synaptic vesicles, which exists in almost all nerve terminals and specifically distributed on the membrane of presynaptic vesicles to participate in the transmission of information between neurons. We found some studies have shown that activation of the BDNF-TrkB signaling pathway following ischemia-reperfusion injury is a critical mechanism underlying the upregulation of SYP expression [25, 26]. BDNF is primarily secreted by neurons and plays a pivotal role in neuronal survival, development, differentiation, synapse formation, and plasticity. BDNF enhances interneuronal connectivity and signal transmission efficiency primarily by promoting neural growth and synaptic plasticity. Research indicates that elevated plasma BDNF levels after neonatal hypoxic-ischemic encephalopathy (HIE) are associated with adverse neurodevelopmental outcomes [27]. BDNF levels in the ipsilateral forebrain of mice with hypoxic-ischemic injury on postnatal day 10 were 1.7- to 2-fold higher than those in sham-operated forebrains, and hypothermia did not attenuate this increase [28]. SYP is mainly transported to the terminal of axon after neuron cell body synthesis, participates in the fusion of synaptic vesicle membrane and presynaptic membrane and neurotransmitter release, and involved in Ca^{2+} binding process, affecting neurotransmitter release and recovery of synaptic vesicles [29, 30], an indicator of nerve injury repair. SYP serves as a more sensitive indicator of synaptic density, distribution, and functional state, while

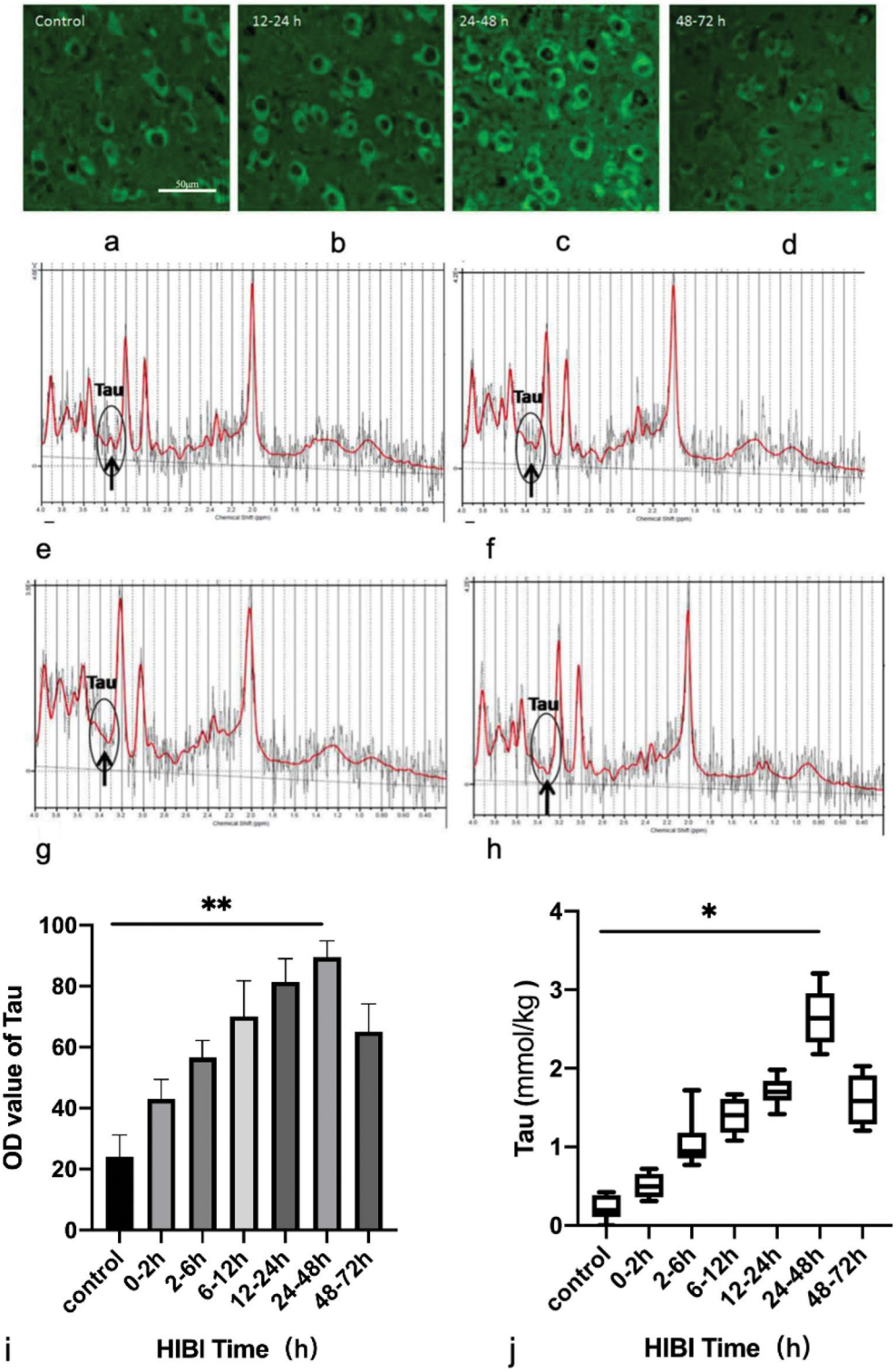

Fig. 3 Immunostaining and ^{1}H-MRS results of Tau protein levels in the basal ganglia region of the control group and model groups at different time points. Immunofluorescence of Tau protein in the control group and at 12–24 h, 24–48 h, and 48–72 h after HI (**a-d**). ^{1}H-MRS spectrum of the right basal segment in the control group (**e**) and at 16 h (**f**), 35 h (**g**), and 68 h (**h**) after HI (processed using LcModel software; Tau peaks shown in the circle are located at approximately 3.25 ppm and 3.42 ppm, as indicated by black arrows). Tau levels increased at 16 h and 35 h after HI and decreased at 68 h. Tau protein concentrations were 0.628 (control), 1.483 (16 h), 2.71 (35 h), and 1.426 (68 h) mmol/kg, respectively. Tau protein exhibited an initial increase followed by a decrease, peaking at 24–48 h after HI, with a significant difference compared to the control group ($P<0.05$). * $P<0.05$, ** $P<0.01$

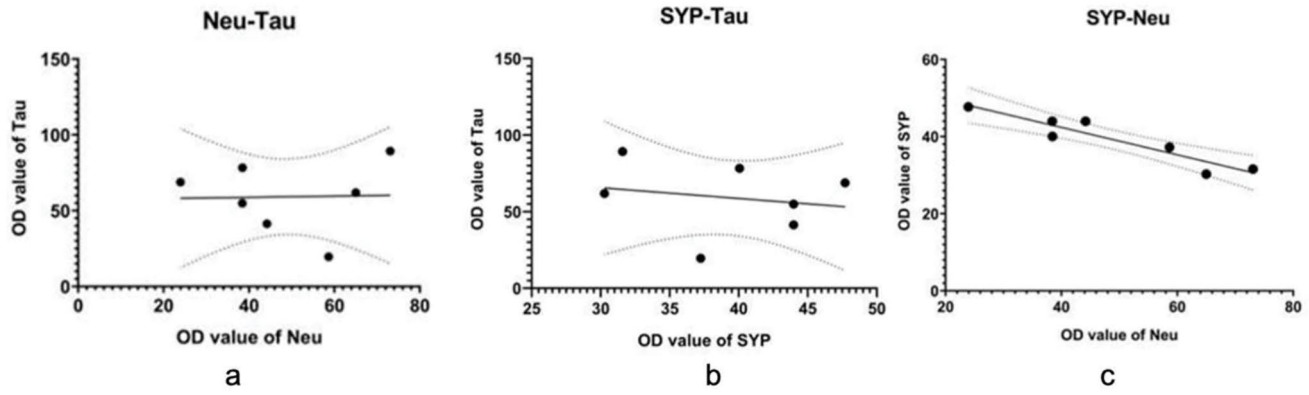

Fig. 4 SYP, Neu, and Tau protein immunostaining. Trends and correlation after HI. Correlations between Neu, SYP, and Tau (immunostaining) are shown in (**a**-**c**), with a significant negative correlation observed between SYP and Neu (**c**) (r = -0.877, P<0.001)

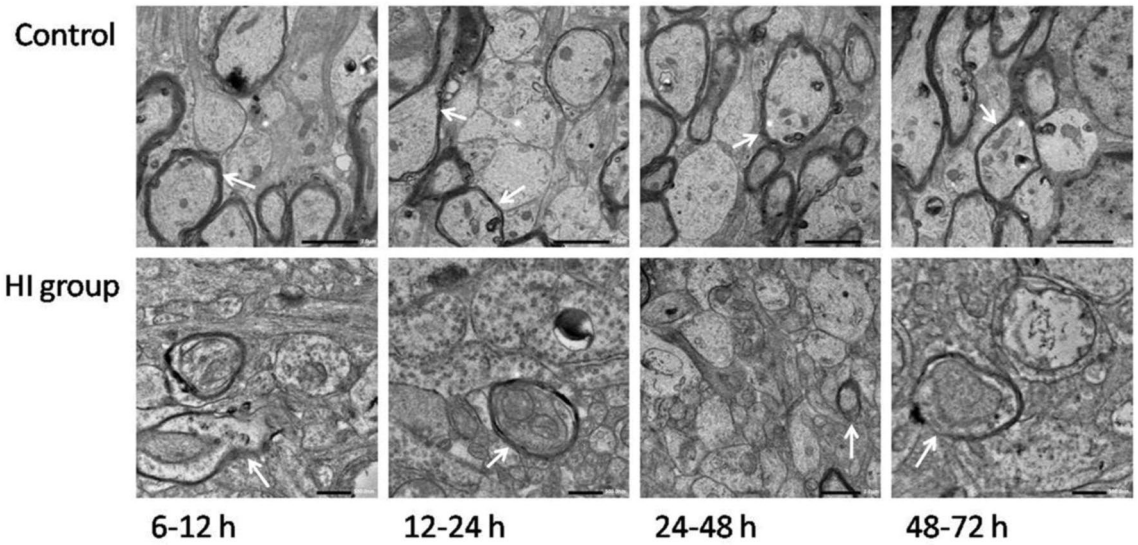

Fig. 5 Myelin electron microscopy images of the control group and various time points after HI. The top row shows the myelin sheath in the control group, which is smooth, uniform, and continuous. The bottom row displays the myelin sheath at various time points after HI, the myelin sheath was uneven and its continuity interrupted. (The structures indicated by white arrows represent the myelin sheath.)

also significantly reflecting changes in synaptic transmission efficiency [31], thus indicating synaptic plasticity [14, 32]. In a murine HI model that SYP levels decreased by 87% at 8 days afterHI, and this deficiency persisted until day 30. However, in neonatal HI (nHI) brain injury models in mice, the temporal acceleration and spatial severity of hippocampal damage often exceed those observed in human HIE patients, making extrapolation of these findings to human HIE pathology uncertain [33]. In contrast, other HI models using neonatal pigs (approximately one week old) exhibit brain injury patterns closely resembling those in human neonates, including high vulnerability of the cortex and basal ganglia, regional damage to white and grey matter, and progressive neuronal injury [34]. Therefore, we selected neonatal pigs as the experimental model to better simulate HI injury in human newborns.

After HI injury, the key to the recovery of nervous system function lies in the restoration of communication between nerve cells and the reconstruction of neural circuits. Studies have shown specific Tau phosphorylation and regulation in the developing brain [18]. High phosphorylation at certain sites is involved in CNS disease in adulthood and necessary for normal brain development. In central degenerative diseases, the pathological role of Tau is mainly reflected in the formation of neurofibrillary tangles (NFTs). However, synaptic damage and loss caused by Tau abnormalities in the fetal brain appear before NFTs and neuronal apoptosis [35], and no study has confirmed the occurrence of NFTs or other pathological Tau changes. Tau-mediated neurotoxicity does not depend on NFT formation; its pathological phosphorylation is sufficient to cause nerve cell damage. One of the pathophysiological mechanisms of HI is brain hypoglycemia. The low glucose metabolism in the HI brain

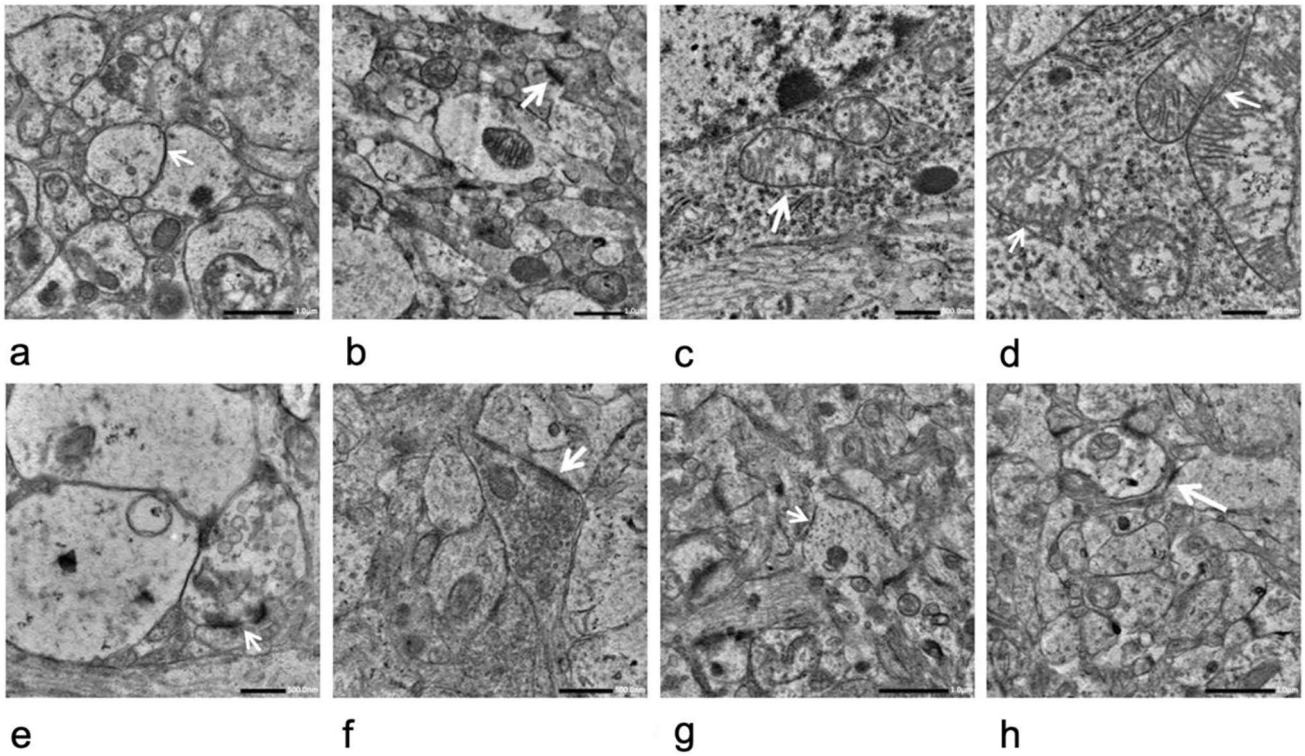

Fig. 6 Synaptic structural changes after HI and control group. Compared with the control group (**a**), at 6–12 h after HI (**b**), the number of synaptic vesicles increased, the thickness of synaptic dense area increased, and normal mitochondria were visible. In the 12–24 h group, the mitochondrial cristae were blurred and the mitochondria swollen (**c**, **d**) (the structures indicated by the white arrow). The thickness of the PSD slightly decreased, with localized interruptions, while the number of synaptic vesicles increased (**e**, **f**). In the 24–48 h group, the number of vesicles and mitochondria decreased, the PSD became thinner, and its continuity was interrupted (**g**, **h**). (Except for images **c** and **d**, the structures indicated by the white arrows represent the PSD area.)

leads to decreased intracellular O-Glcnac glycosylation and increased Tau phosphorylation; the two are negatively correlated [36, 37]. Hypoglycemia caused by cerebral ischemia can lead to abnormal Tau phosphorylation. A study have shown elevated Tau levels in the umbilical cord blood of neonates with HIE and in the white matter of HI model mice [38, 39]. After HI, a large accumulation of extracellular glutamate and glutamate receptors continue to activate, mediating Ca^{2+} influx, activating CaMK II, MAPK, and other pathways to cause Tau hyperphosphorylation [40]. Hyperphosphorylated Tau can cause mitochondrial dysfunction, which leads to energy metabolism disorders of OL and neurons.

This study found that SYP and Tau immunostaining increased first and then decreased after HI, but their peaks occurred at different times; there was no correlation between the two. The increase in Tau may be caused by the increased reactive expression of Tau protein expressed by OL after HI. Simultaneously, after neuron injury, Tau can be released from the neuronal cell body and can be shed from microtubules. Therefore, the more damaged cells and the more severe the injury, the more Tau protein will be released and the more free Tau, leading to increased Tau content in brain tissue. The subsequent slight Tau decrease may be caused by nerve cell death after HI and limited Tau synthesis. Therefore, changes in Tau protein expression underlie nerve cell degeneration [41], which play a role in regulating synaptic plasticity and cytoskeletal dynamics. The increased SYP after HI indicated that the nervous system after HI was in the compensatory stage and nerve repair is active, mainly because brain tissue is very sensitive to hypoxia and ischemia injury. After blocking the cerebral blood flow of newborn pigs, a series of cascade reactions in brain tissues, started synaptic regeneration through neurohumoral regulation and neuro-endocrine-immune action, consistent with increased Tau expression for promoting myelination after HI [42]. With increasing time after HI, SYP decreased significantly, suggesting decrease synaptic vesicle transport in the region and indicating that hypoxia and ischemia led to reduced synaptic density and synaptic function damage in the region. This may be caused by insufficient SYP synthesis due to energy failure of some nerve cells, a mechanism of brain hypoxia and ischemia leading to neurological damage. Simultaneously, it was consistent with the decreased Tau and myelin regeneration in the late HI period. SYP and Tau expression increased first and then decreased after HI,

reflecting the plasticity of the nervous system after HI and the pathophysiological changes of nerve cell necrosis after late decompensation.

Marques et al. investigated the effects of prenatal hypoxic-ischemic (HI) injury in rats on depressive-like behaviors and synaptic plasticity in the prefrontal cortex (PFC). They analyzed synaptic protein alterations in prenatal HI model rats 45 days after birth and demonstrated that HI injury led to reduced neuronal counts in the PFC, decreased SYP and PSD-95 expression, with more pronounced damage in male mice compared to females [43]. In our study, at 6–12 h after HI injury, TEM showed a thickened synaptic dense area, the mitochondrial morphology was normal, and the number of vesicles slightly increased, indicating nerve repair in the post-compensatory phase of HI, manifested as synaptic regeneration and increased presynaptic vesicle transport, consistent with the increased SYP and Tau expression. The transient increase in SYP and elevated number of presynaptic vesicles at 6–12 h after HI suggest partial synaptic recovery during this phase, demonstrating synaptic plasticity in the compensatory period of the HI-injured nervous system and indicating rapid initiation of neural repair without intervention. From 12 to 24 h after HI, mitochondrial swelling and blurred cristae were observed, indicating impaired energy metabolism. At this time point, transmission electron microscopy (TEM) revealed an increased number of synaptic vesicles, while SYP protein was reduced compared to the 6–12 h group. This phenomenon may result from a fusion barrier between synaptic vesicles and the presynaptic membrane, leading to vesicle entrapment within the presynaptic terminal, which is associated with long-term potentiation (LTP)-induced synaptic morphological changes and enhanced membrane recycling [44]. PSD thickness was thinner, indicating weaker synaptic connection between cells. Vesicle reduction, interruption of PSD continuity, widening of the synaptic gap, and reduction of the number of mitochondria after 48–72 h after HI indicated energy exhaustion and irreversible synaptic damage. Thus, HI can reflect synaptic plasticity by influencing the expression of postsynaptic proteins.

Neu is a specific protein secreted by neurons, expressed during development and reduces or disappears after maturation. Under normal physiological conditions, Neu mainly inhibits disordered axon growth and induces nerve fibers to project to the right target cells [45]. In this study, Neu immunostaining was first down-regulated and then up-regulated after nervous system injury, which was negatively correlated with SYP immunostaining trends. This down-regulation may facilitate axonal growth and elongation, enabling connections to appropriate target cells, combined with the SYP and Tau increase and PSD thickening, which reflects CNS plasticity during the compensatory period after HI. However, activated glial cells after brain injury also secreted a large amount of Neu [46], over time, reperfusion injury and Neu's inhibitory may effect on axon growth further damaged axons inhibiting synaptic formation. At this time, SYP and Tau immunostaining decreased, suggesting neural system plasticity decompensation. After 24–48 h, Neu decreased again, which suggested decreased neuronal Neu synthesis and reflected neuronal damage.

This study elucidates the dynamic changes of Tau protein, synaptophysin (SYP), and neurocan (Neu) in neuroplasticity following hypoxic-ischemic (HI) brain injury, offering potential therapeutic targets, biomarkers, and critical therapeutic time windows. It provides a theoretical foundation for the diagnosis, prognostic evaluation, and neuroprotective strategies of neonatal HIE, while also proposing a reference direction for developing multi-target combination therapies. These findings hold significant potential for translational applications in clinical practice.

Conclusion

The key to the recovery of nervous system function lies in the restoration of communication between nerve cells and the reconstruction of neural circuits. After HI injury, the nervous system triggers neuroprotective mechanisms to adapt to pathological conditions. Tau protein, axon-myelin sheath, synaptic associated protein, and synaptic structures jointly affect and regulate CNS plasticity after HI; these factors complete the information and material exchange of the nervous system.

Acknowledgements This work was supported by the National Natural Science Foundation of China (NO.81871408), National Science Foundation for Young Scientists of China (NO.81801658), Outstanding Scientific Fund of Shengjing Hospital (NO. 201402) and 345 Talent Project of Shengjing Hospital.

Author Contributions Y.Z provided administrative support and study materials. S.Z collected and assembled the data, and all authors conducted data analysis and interpretation. All authors contributed to the conception, design, and writing of the manuscript, and all authors approved the final version of the manuscript.

Data Availability The data that support the findings of this study are available from the corresponding author upon reasonable request.

Declarations

Competing Interests The authors declare no competing interests.

References

1. Sebastian-Serrano A, de Diego-Garcia L, Diaz-Hernandez M (2018) The neurotoxic role of extracellular Tau protein. Int J Mol Sci. https://doi.org/10.3390/ijms19040998
2. Sierra A, Beccari S, Diaz-Aparicio I, Encinas JM, Comeau S, Tremblay ME (2014) Surveillance, phagocytosis, and inflammation: how never-resting microglia influence adult hippocampal neurogenesis. Neural Plast 2014:610343. https://doi.org/10.1155/2014/610343
3. Zheng Y, Wang XM (2018) Expression changes in lactate and glucose metabolism and associated transporters in basal ganglia following Hypoxic-Ischemic reperfusion injury in piglets. AJNR Am J Neuroradiol 39:569–576. https://doi.org/10.3174/ajnr.A5505
4. Zhang Y, Xiang Z, Jia Y, He X, Wang L, Cui W (2019) The Notch signaling pathway inhibitor Dapt alleviates autism-like behavior, autophagy and dendritic spine density abnormalities in a valproic acid-induced animal model of autism. Prog Neuropsychopharmacol Biol Psychiatry 94:109644. https://doi.org/10.1016/j.pnpbp.2019.109644
5. Valtorta F, Pennuto M, Bonanomi D, Benfenati F (2004) Synaptophysin: leading actor or walk-on role in synaptic vesicle exocytosis? BioEssays 26:445–453. https://doi.org/10.1002/bies.20012
6. Lu B, Chow A (1999) Neurotrophins and hippocampal synaptic transmission and plasticity. J Neurosci Res 58:76–87
7. Perrone-Capano C, Volpicelli F, Penna E, Chun JT, Crispino M (2021) Presynaptic protein synthesis and brain plasticity: from physiology to neuropathology. Prog Neurobiol 202:102051. https://doi.org/10.1016/j.pneurobio.2021.102051
8. Citri A, Malenka RC (2008) Synaptic plasticity: multiple forms, functions, and mechanisms. Neuropsychopharmacology 33:18–41. https://doi.org/10.1038/sj.npp.1301559
9. Yang Z, Levison SW (2007) Perinatal hypoxic/ischemic brain injury induces persistent production of striatal neurons from subventricular zone progenitors. Dev Neurosci 29:331–340. https://doi.org/10.1159/000105474
10. Buono KD, Goodus MT, Guardia Clausi M, Jiang Y, Loporchio D, Levison SW (2015) Mechanisms of mouse neural precursor expansion after neonatal hypoxia-ischemia. J Neuroscience: Official J Soc Neurosci 35:8855–8865. https://doi.org/10.1523/JNEUROSCI.2868-12.2015
11. Ziemka-Nalecz M, Janowska J, Strojek L, Jaworska J, Zalewska T, Frontczak-Baniewicz M, Sypecka J (2018) Impact of neonatal hypoxia-ischaemia on oligodendrocyte survival, maturation and myelinating potential. J Cell Mol Med 22:207–222. https://doi.org/10.1111/jcmm.13309
12. Rocha-Ferreira E, Hristova M (2016) Plasticity in the neonatal brain following Hypoxic-Ischaemic injury. Neural Plast 2016:4901014. https://doi.org/10.1155/2016/4901014
13. Cousin MA (2021) Synaptophysin-dependent synaptobrevin-2 trafficking at the presynapse-Mechanism and function. J Neurochem 159:78–89. https://doi.org/10.1111/jnc.15499
14. Xie Z, Long J, Liu J, Chai Z, Kang X, Wang C (2017) Molecular mechanisms for the coupling of endocytosis to exocytosis in neurons. Front Mol Neurosci 10:47. https://doi.org/10.3389/fnmol.2017.00047
15. Yadav L, Babu MK, Das K, Mohanty S, Divya P, Shankar G, Kini U (2017) Role of synaptophysin in the intraoperative assessment of quadrantic innervation of the proximal doughnut in hirschsprung disease. Natl Med J India 30:187–192. https://doi.org/10.4103/0970-258X.218669
16. Shen LH, Li Y, Gao Q, Savant-Bhonsale S, Chopp M (2008) Down-regulation of neurocan expression in reactive astrocytes promotes axonal regeneration and facilitates the neurorestorative effects of bone marrow stromal cells in the ischemic rat brain. Glia 56:1747–1754. https://doi.org/10.1002/glia.20722
17. Sheng M, Kim E (2011) The postsynaptic organization of synapses. Cold Spring Harb Perspect Biol 3. https://doi.org/10.1101/cshperspect.a005678
18. Yu Y, Run X, Liang Z, Li Y, Liu F, Liu Y, Iqbal K, Grundke-Iqbal I, Gong CX (2009) Developmental regulation of Tau phosphorylation, Tau kinases, and Tau phosphatases. J Neurochem 108:1480–1494. https://doi.org/10.1111/j.1471-4159.2009.05882.x
19. Wu Q, Ge W, Chen Y, Kong X, Xian H (2019) PKM2 involved in neuronal apoptosis on Hypoxic-ischemic encephalopathy in neonatal rats. Neurochem Res 44:1602–1612. https://doi.org/10.1007/s11064-019-02784-7
20. Klein C, Kramer EM, Cardine AM, Schraven B, Brandt R, Trotter J (2002) Process outgrowth of oligodendrocytes is promoted by interaction of Fyn kinase with the cytoskeletal protein Tau. J Neuroscience: Official J Soc Neurosci 22:698–707
21. Reynolds CH, Garwood CJ, Wray S, Price C, Kellie S, Perera T, Zvelebil M, Yang A, Sheppard PW, Varndell IM, Hanger DP, Anderton BH (2008) Phosphorylation regulates Tau interactions with Src homology 3 domains of phosphatidylinositol 3-kinase, phospholipase Cgamma1, Grb2, and Src family kinases. J Biol Chem 283:18177–18186. https://doi.org/10.1074/jbc.M709715200
22. De Gois S, Schafer MK, Defamie N, Chen C, Ricci A, Weihe E, Varoqui H, Erickson JD (2005) Homeostatic scaling of vesicular glutamate and GABA transporter expression in rat neocortical circuits. J Neuroscience: Official J Soc Neurosci 25:7121–7133. https://doi.org/10.1523/JNEUROSCI.5221-04.2005
23. Mochida S (2020) Neurotransmitter release site replenishment and presynaptic plasticity. Int J Mol Sci 22. https://doi.org/10.3390/ijms22010327
24. Kusick GF, Chin M, Raychaudhuri S, Lippmann K, Adula KP, Hujber EJ, Vu T, Davis MW, Jorgensen EM, Watanabe S (2020) Synaptic vesicles transiently dock to refill release sites. Nat Neurosci 23:1329–1338. https://doi.org/10.1038/s41593-020-00716-1
25. Lu B, Nagappan G, Lu Y (2014) BDNF and synaptic plasticity, cognitive function, and dysfunction. Handb Exp Pharmacol 220:223–250. https://doi.org/10.1007/978-3-642-45106-5_9
26. Zhu X, Han S, Geng Y, Ren W, Quan F (2024) Brain-Derived neurotrophic Factor-TrkB pathway on synaptic plasticity in ischemic stroke rats. Int Heart J 65:1095–1106. https://doi.org/10.1536/ihj.24-312
27. Dietrick B, Molloy E, Massaro AN, Strickland T, Zhu J, Slevin M, Donoghue V, Sweetman D, Kelly L, O'Dea M, McGowan M, Vezina G, Glass P, Vaidya D, Brooks S, Northington F, Everett AD (2020) Plasma and cerebrospinal fluid candidate biomarkers of neonatal encephalopathy severity and neurodevelopmental outcomes. J Pediatr 226:71–79e75. https://doi.org/10.1016/j.jpeds.2020.06.078
28. Diaz J, Abiola S, Kim N, Avaritt O, Flock D, Yu J, Northington FJ, Chavez-Valdez R (2017) Therapeutic hypothermia provides

variable protection against behavioral deficits after neonatal Hypoxia-Ischemia: A potential role for Brain-Derived neurotrophic factor. Dev Neurosci 39:257–272. https://doi.org/10.1159/000454949
29. Davies HA, Kelly A, Dhanrajan TM, Lynch MA, Rodriguez JJ, Stewart MG (2003) Synaptophysin Immunogold labelling of synapses decreases in dentate gyrus of the hippocampus of aged rats. Brain Res 986:191–195. https://doi.org/10.1016/s0006-8993(03)03251-7
30. Himeda T, Mizuno K, Kato H, Araki T (2005) Effects of age on immunohistochemical changes in the mouse hippocampus. Mech Ageing Dev 126:673–677. https://doi.org/10.1016/j.mad.2004.12.004
31. Zhu X, Wang P, Liu H, Zhan J, Wang J, Li M, Zeng L, Xu P (2019) Changes and significance of SYP and GAP-43 expression in the Hippocampus of CIH rats. Int J Med Sci 16:394–402. https://doi.org/10.7150/ijms.28359
32. Kwon SE, Chapman ER (2011) Synaptophysin regulates the kinetics of synaptic vesicle endocytosis in central neurons. Neuron 70:847–854. https://doi.org/10.1016/j.neuron.2011.04.001
33. Chavez-Valdez R, Lechner C, Emerson P, Northington FJ, Martin LJ (2021) Accumulation of PSA-NCAM marks nascent neurodegeneration in the dorsal hippocampus after neonatal hypoxic-ischemic brain injury in mice. J Cereb Blood Flow Metab 41:1039–1057. https://doi.org/10.1177/0271678x20942707
34. Koehler RC, Yang ZJ, Lee JK, Martin LJ (2018) Perinatal hypoxic-ischemic brain injury in large animal models: relevance to human neonatal encephalopathy. J Cereb Blood Flow Metab 38:2092–2111. https://doi.org/10.1177/0271678x18797328
35. Yoshiyama Y, Higuchi M, Zhang B, Huang SM, Iwata N, Saido TC, Maeda J, Suhara T, Trojanowski JQ, Lee VM (2007) Synapse loss and microglial activation precede tangles in a P301S tauopathy mouse model. Neuron 53:337–351. https://doi.org/10.1016/j.neuron.2007.01.010
36. Liu F, Iqbal K, Grundke-Iqbal I, Hart GW, Gong CX (2004) O-GlcNAcylation regulates phosphorylation of Tau: a mechanism involved in Alzheimer's disease. Proc Natl Acad Sci USA 101:10804–10809. https://doi.org/10.1073/pnas.0400348101
37. Liu Y, Liu F, Iqbal K, Grundke-Iqbal I, Gong CX (2008) Decreased glucose transporters correlate to abnormal hyperphosphorylation of Tau in alzheimer disease. FEBS Lett 582:359–364. https://doi.org/10.1016/j.febslet.2007.12.035
38. Tarkowska A, Furmaga-Jabłońska W, Bogucki J, Kocki J, Pluta R (2023) Preservation of biomarkers associated with Alzheimer's disease (Amyloid peptides 1–38, 1–40, 1–42, Tau protein, Beclin 1) in the blood of neonates after perinatal asphyxia. Int J Mol Sci. https://doi.org/10.3390/ijms241713292
39. Zhang Y, Wang Y, Dou H, Wang S, Qu D, Peng X, Zou N, Yang L (2024) Caffeine improves mitochondrial dysfunction in the white matter of neonatal rats with hypoxia-ischemia through deacetylation: a proteomic analysis of lysine acetylation. Front Mol Neurosci 17:1394886. https://doi.org/10.3389/fnmol.2024.1394886
40. Paoletti P, Bellone C, Zhou Q (2013) NMDA receptor subunit diversity: impact on receptor properties, synaptic plasticity and disease. Nat Rev Neurosci 14:383–400. https://doi.org/10.1038/nrn3504
41. Trivellato D, Munari F, Assfalg M, Capaldi S, D'Onofrio M (2024) Untangling the complexity and impact of Tau protein ubiquitination. ChemBioChem 25:e202400566. https://doi.org/10.1002/cbic.202400566
42. Mueller RL, Combs B, Alhadidy MM, Brady ST, Morfini GA, Kanaan NM (2021) Tau: A signaling hub protein. Front Mol Neurosci 14:647054. https://doi.org/10.3389/fnmol.2021.647054
43. Marques KL, Moreira ML, Thiele MC, Cunha-Rodrigues MC, Barradas PC (2023) Depressive-like behavior and impaired synaptic plasticity in the prefrontal cortex as later consequences of prenatal hypoxic-ischemic insult in rats. Behav Brain Res 452:114571. https://doi.org/10.1016/j.bbr.2023.114571
44. Toni N, Buchs PA, Nikonenko I, Povilaitite P, Parisi L, Muller D (2001) Remodeling of synaptic membranes after induction of long-term potentiation. J Neurosci 21:6245–6251. https://doi.org/10.1523/jneurosci.21-16-06245.2001
45. Miyata S, Kitagawa H (2015) Mechanisms for modulation of neural plasticity and axon regeneration by chondroitin sulphate. J Biochem 157:13–22. https://doi.org/10.1093/jb/mvu067
46. Schwarzacher SW, Vuksic M, Haas CA, Burbach GJ, Sloviter RS, Deller T (2006) Neuronal hyperactivity induces astrocytic expression of neurocan in the adult rat hippocampus. Glia 53:704–714. https://doi.org/10.1002/glia.20329